Nuclear microprobe investigation into the trace elemental contents of carotid artery walls of apolipoprotein E deficient mice

Ren Minqin [a,b,*], Huang En [b], Konstanze Beck [c], Reshmi Rajendran [a,b], Ben J. Wu [c], Barry Halliwell [b], Frank Watt [a], Roland Stocker [c]

[a] *Department of Physics, Centre for Ion Beam Applications, National University of Singapore, Singapore 117542, Singapore*
[b] *Department of Biochemistry of National University of Singapore, Singapore 117542, Singapore*
[c] *Centre for Vascular Research, University of New South Wales, Sydney, Australia*

Available online 14 February 2007

Abstract

Atherosclerosis is a progressive disease that causes lesions in large and medium-sized arteries. There is increasing evidence that the function of vascular endothelial cells is impaired by oxidation reactions, and that metal ions may participate in these processes. The nuclear microscopy facility in NUS, which has the ability to focus a 2 MeV proton beam down to sub micron spot sizes, was used to investigate the trace elemental changes (e.g. Zn and Fe) in atherosclerotic lesions in the common carotid artery of apolipoprotein E deficient mice fed a high fat diet. In this preliminary study, which is part of a larger study to investigate the effects of probucol on carotid artery atherosclerosis, two sets of mice were used; a test set fed a high fat diet +1% probucol, and a control set which was fed a high fat diet only.

The results show that the Zn/Fe ratio was significantly higher in the media of arteries of probucol treated animals without overlying lesion (4.3) compared to the media with overlying lesion (1.3) ($p = 0.004$) for test mice. For the control mice, the arterial Zn/Fe ratio was 1.8 for media without overlying lesion, compared with 1.0 for media with overlying lesion ($p = 0.1$). Thus, for media without overlying lesion, the Zn/Fe ratio was significantly higher ($p = 0.009$) in probucol-treated (4.3) than control mice (1.8), whereas there was little difference in the ratios between the two groups in media with overlying lesion (1.3 compared with 1.0).

These preliminary results are consistent with the idea that the levels of iron and zinc concentrations within the artery wall may influence the formation of atherosclerotic plaque in the carotid artery.

1. Introduction

Atherosclerosis is characterized by the accumulation of cholesterol deposits in macrophages in large- and medium-sized arteries. This deposition leads to a proliferation of certain cell types within the arterial wall that gradually impinge upon the vessel lumen and impede blood flow.

There is now also a consensus that atherosclerosis represents a state of heightened oxidative stress characterized by lipid and protein oxidation in the vascular wall [1]. The administration of hypolipidemic drugs and antioxidants is, therefore, a rational means of trying to prevent the development of atherosclerosis.

Apolipoprotein E-deficient (apoE$^{-/-}$) mice are commonly used as a model of hypercholesterolemia-induced atherosclerosis [2]. Apolipoprotein E is a component of three plasma lipoproteins – chylomicron remnants (CMr) very low-density lipoprotein (VLDL) and high-density lipoprotein (HDL). It is a ligand for many receptors –

---

* Corresponding author. Address: Department of Physics, Centre for Ion Beam Applications, National University of Singapore, Singapore 117542, Singapore. Tel.: +65 65162638; fax: +65 67776126.
  E-mail address: phyrenmq@nus.edu.sg (R. Minqin).

the LDL receptors, the VLDL receptor and the LDL receptor related protein (LRP) and megalin (gp 330). It is thus closely involved in the clearance of many lipoproteins most notably CMr and VLDL. The genetic removal of the apoE gene in mice results in profound hyperlipoproteinemia, affecting most remnants and VLDL. ApoE deficient mice spontaneously develop severe atherosclerosis that shows many features of the disease in humans [3,4].

Probucol is a lipid soluble antioxidant and cholesterol-lowering drug that attenuates atherogenesis in animals and humans and that protects human coronary arteries from restenosis. Several protective functions likely contribute to the protection offered by probucol, including anti-inflammatory activity, the promotion of re-endothelialization, inhibition of smooth muscle cell proliferation, and the protection of endothelial cell integrity [5].

Endothelial dysfunction is accepted as a surrogate marker of vascular pathology leading to atherosclerosis. Studies also indicate that zinc is vital to vascular endothelial cell integrity and zinc deficiency causes severe impairment of the endothelial barrier function [6–9]. Our previous study in rabbits showed that iron concentrations appear to correlate positively with the extent of lesion development and that zinc is inversely correlated with the atherosclerotic lesion formation [10]. It is possible that iron is pro-oxidative whereas zinc may antagonize any early lesion formation accelerated by free radical production caused by increased iron levels. The ratio of zinc to iron concentrations therefore may be a useful indicator of atherosclerosis progression.

As part of a larger study carried out on the protective property of probucol on atherosclerosis, we have used nuclear microscopy to investigate the trace elemental contents of the carotid artery walls of apoE-deficient mice.

2. Materials and methods

2.1. Materials

Male apoE$^{-/-}$ mice purchased from Animal Resources Centre (Perth, Australia) were used at 8–10 weeks of age, and then fed for 24 weeks ad libitum a high-fat diet containing 21.2 (w/w) fat and 0.15% (w/w) cholesterol (specifications of the Harlan Teklad diet TD88137) prior to culling. Seven carotid arteries from the control animals on high fat diet and animals fed a high fat diet supplemented with 1% (w/w) probucol were used.

Common carotid arteries were resected from animals following perfusion under near physiological pressure (∼100 mm Hg) with Dulbecco's phosphate-buffered saline containing 20 μM butylated hydroxytoluene and 1 mM ethylenediaminetetraacetic acid as described previously [11]. Immediately after resection, arteries were placed in phosphate-buffered saline containing 30% sucrose and stored overnight at 4 °C. The next day, cold arteries were placed into plastic moulds containing Tissue-tek (ProSci-Tech, Thuringowa, Qld, Australia) and the moulds then

transferred into a beaker containing 2-methyl-butane previously cooled in liquid nitrogen. Once the Tissue-tek solution appeared frozen, moulds containing the arteries were transferred onto dry ice, wrapped in aluminium foil and then stored at −80 °C before sectioning.

This study was approved by the local Animal Care and Use Committee.

2.2. Histochemistry and nuclear microscopy analysis

Carotid artery samples were sectioned (14 μm thick sections) using a Leica CM3050S cryostat. The sectioning started at the distal end gradually moving downwards in 10-μm steps, and as soon as the start of bifurcation was reached (see the reference point in Fig. 1), 14-μm sections were cut and picked up on pioloform coated aluminium target holders for nuclear microscopy analysis and imaging [10]. Serial sections were also cut and mounted on gelatin-coated slides for hematoxylin and eosin staining in order to monitor the lesion development and measure the lesion area. This analysis was carried out using the Carl Zeiss Axiophot 2 image analyzer utilizing the KS400 (version 3.18) analysis software. Subsequently sections at 100 μm, 200 μm, 300 μm, 400 μm and to 500 μm (below the bifurcation point) were taken in order to investigate thoroughly how the lesion develops along the common carotid artery (the results will be presented elsewhere).

Sections taken at the bifurcation reference point were scanned using the National University of Singapore nuclear microscopy facility operating with a 2.1 MeV proton beam focused to a spot size of approximately 1 μm^2 and with a beam current of 400–500 pA on average [12]. Techniques combining scanning transmission ion microscopy (STIM), Particle induced X-ray emission (PIXE) and Rutherford backscattering spectrometry (RBS) were employed simultaneously in the analysis. The area of interest was positioned using the structure and density information provided by STIM. Quantitative results were determined by RBS and PIXE: RBS provides information on matrix composition and incident charge; PIXE was used for measuring the concentrations of the elements from sodium upwards in the periodic table. X-rays of different elements were detected simultaneously using a lithium-drifted silicon X-ray detector placed at 90° to the beam axis and fitted with a filter designed for optimal detection of trace elements such as iron and zinc in biological specimens.

3. Results and discussion

The bifurcation of the common carotid artery is the point at which the artery divides into external and internal carotid arteries, and a region highly susceptible to atherosclerosis because of much higher wall stress compared to other regions [13]. The sections taken from the bifurcation of all carotid artery samples were analyzed. Eight out of 13 samples had lesions of size ranging from 21% to 78%
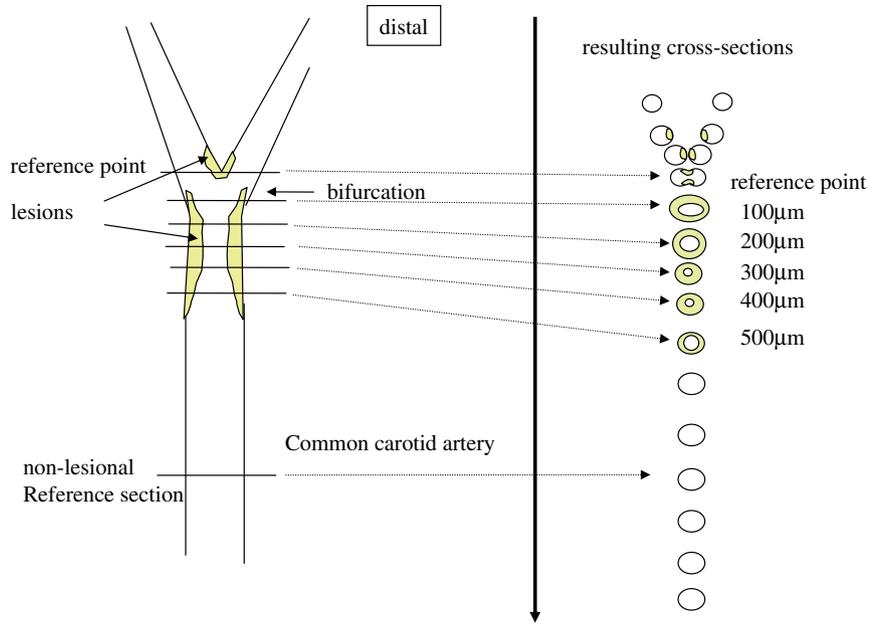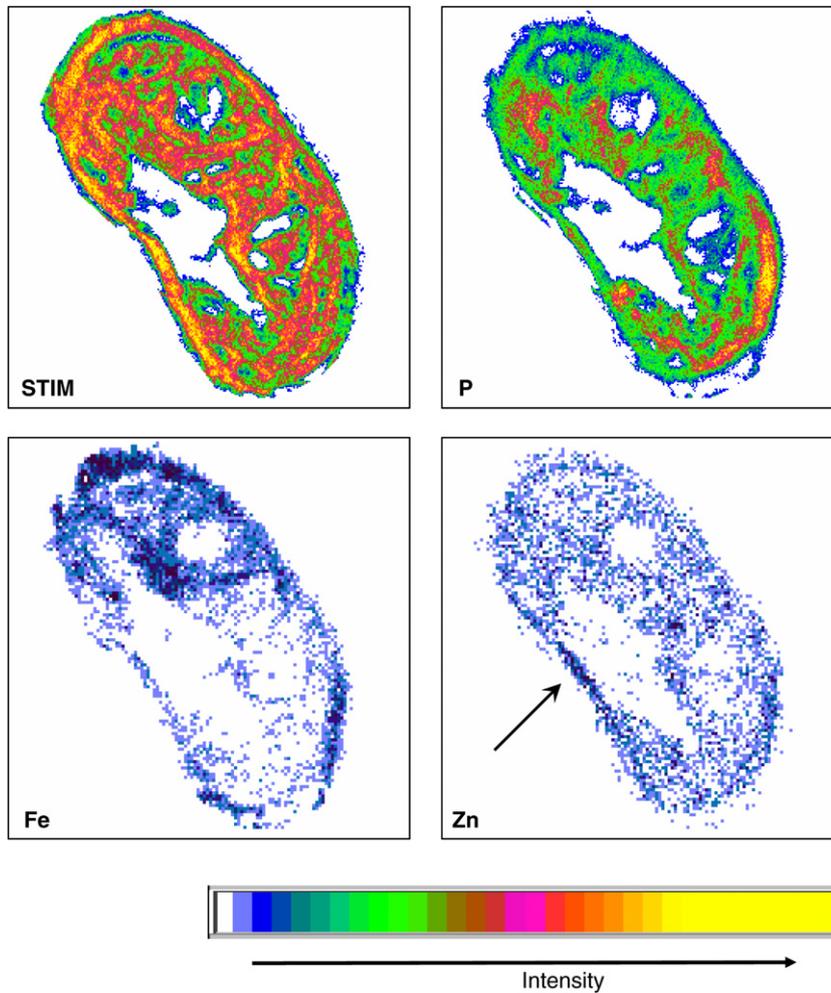
Fig. 1. Direction of cross-sectioning.

Fig. 2. STIM image and elemental maps of one of the bifurcation point sections.

(percentage of lesion to the whole lumen area); one section from a control mouse was damaged during the sample preparation and therefore not used. Of the 8 arteries which exhibited lesions, 5 were from control and 3 from probucol-treated animals. Most of the plaques were well advanced with a well-defined fibrous cap. Fig. 2 shows the STIM image and elemental maps of a bifurcation section of one of the arteries from the control group. The STIM map was collected within the first few minutes of the 4 h run (using a proton beam current of 600 pA), which enables us to position the region of interest in a couple of minutes. The STIM signal was disconnected to avoid significant dead time in the OMDAQ data collection system during the analysis phase. The phosphorus map revealed a clear boundary between neointima and underlying media which made distinction between diseased (i.e. neointima) and apparently non-diseased arterial wall material (media) possible. The elemental maps clearly showed that the Zn content was higher in the media without overlying lesions (indicated by arrow in Fig. 2) whilst Fe was often, although not always, more abundant in the media with overlying lesions. The results shown in Fig. 2 are representative for all samples, although the mean lesion size was smaller in arteries from probucol-treated than control animals (data not shown).

All 13 carotid artery sections taken at the bifurcation reference point were analyzed for elemental concentrations. For each section that contained plaque (5 controls and 3 probucol), 2 regions of artery wall were selected for further analysis: one region of media with overlying lesion and one without overlying lesion. For each of the remaining sections which did not exhibit plaques, 2 independent regions of the artery wall were chosen. All selected regions were subjected to nuclear microscopy analysis. Average elemental concentrations (in parts per million) of the selected

regions are shown in Table 1. Zinc concentrations were observed to be highest in sections obtained from probucol-treated animals and in media without overlying plaque, whereas zinc levels were much lower in the media with overlying plaque in sections from both control and probucol-treated animals. Iron was found to be the highest in the media with overlying lesion in the control group and lowest in the media without overlying plaque in the probucol group. In arteries from probucol-treated mice, medial iron content was lower compared to that in control mice, irrespective of the presence of overlying lesion (Table 1).

The Zn/Fe ratios were also calculated (Table 2). As can be seen, this ratio was significantly higher in the media of arteries of probucol-treated animals without overlying lesion (4.3) compared to the media with overlying lesion (1.3) ($p = 0.004$). For *control mice*, the arterial Zn/Fe ratio was 1.8 for media without overlying lesion, compared with 1.0 for media with overlying lesion ($p = 0.1$). Thus, for media without overlying lesion, the Zn/Fe ratio was signif-

Table 2
Zinc to iron ratio of two measured artery walls areas for all the carotid artery samples (artery-1: media without overlying lesion, artery-2: media with overly lesion)

Probucol	Zn/Fe ratio		Control	Zn/Fe ratio	
	Artery-1	Artery-2		Artery-1	Artery-2
CA-3	5.60		CA-1	1.94	0.18
CA-4	6.78		CA-2	2.19	0.73
CA-5	4.23		CA-10	1.90	2.22
CA-6	5.67	1.30	CA-11	0.55	0.72
CA-7	3.09		CA-12	1.95	1.19
CA-8	2.21	1.25	CA-13	2.33	
CA-9	2.50	1.21			
Average	4.30	1.26	Average	1.81	1.01
Std error	0.62	0.02	Std error	0.24	0.31

Table 1
Elemental concentration of artery areas of carotid artery samples (in parts per million, and error in brackets)

Control	Ca		Fe		Zn		Probucol	Ca		Fe		Zn	
Media without overlying lesion													
CA-1	103	(3)	17	(1)	33	(2)	CA-3	80	(4)	10	(1)	42	(3)
CA-2	122	(3)	21	(1)	46	(2)	CA-4	87	(6)	6	(1)	37	(4)
CA-10	61	(5)	10	(2)	19	(3)	CA-5	118	(5)	10	(1)	37	(4)
CA-11	122	(5)	20	(2)	11	(2)	CA-6	67	(5)	6	(1)	34	(4)
CA-12	125	(6)	19	(2)	37	(4)	CA-7	73	(2)	11	(1)	34	(1)
CA-13	86	(4)	18	(1)	34	(3)	CA-8	124	(6)	19	(2)	42	(4)
							CA-9	107	(7)	24	(2)	60	(5)
Average	103		18		30		Average	94		12		41	
Std error	10		2		5		Std error	10		2		3	
Media with overlying lesion													
CA-1	123	(3)	76	(2)	14	(2)							
CA-2	249	(3)	62	(1)	45	(1)							
CA-10	99	(5)	9	(1)	20	(2)	CA-6	82	(5)	23	(2)	30	(4)
CA-11	78	(4)	18	(1)	13	(2)	CA-8	111	(5)	20	(1)	25	(2)
CA-12	105	(5)	31	(2)	37	(2)	CA-9	75	(5)	14	(1)	17	(3)
Average	131		39		26		Average	89		19		24	
Std error	27		12		6		Std error	9		2		3	

icantly higher ($p = 0.009$) in probucol-treated (4.3) than control mice (1.8), whereas there was little difference in the ratios between the two groups in media with overlying lesion (1.3 compared with 1.0).

These results show the same trend as observed in the aorta of cholesterol-fed rabbits where relatively high concentrations of iron are associated with atherosclerotic lesions, whereas high levels of zinc were present in aortas with comparatively less disease [10].

Nuclear microscopy is able to simultaneously extract other elemental data, and calcium data is also included in Table 1. We did not observe any significant difference in calcium levels in the present study, whereas in previous rabbit studies [10,14], we observed an increase in calcium concentrations in diseased artery walls.

4. Conclusion

Although the results on carotid artery samples are preliminary and only a small part of a larger study, there appears to be a consistent trend similar to our previous studies carried out on atherosclerosis using rabbit models [10,14,15], in that high concentrations of localised iron are associated with increased atherosclerosis, whereas high levels of zinc are associated with inhibition of disease.

A novel observation in the present study is that probucol appears to increase the Zn concentration and the Zn/Fe ratio in carotid arteries of ApoE$^{-/-}$ mice. The underlying reasons for this remain to be investigated, although it is interesting to note in this context that probucol has been reported previously to inhibit the fall in serum Zn level induced by intravenous injection of lipopolysaccharide in zymosan-primed mice [16]. Clearly it will be important to establish whether alterations in the relative arterial concentrations of Zn and Fe are a consequence or cause of atherosclerosis. In support of a causative inverse relationship between Zn concentrations and atherosclerosis, a recent independent study has shown that zinc supplementation significantly retards the development of lesion formation in rabbit aorta [17]. A parallel study on the ability of probucol in reducing remodelling in response to plaque growth resulting in lumen compromise is also in press [18].

In summary, our results have shown that nuclear microscopy has the ability to image the morphology of biological tissue (and cells) and map trace elements such as Ca, Fe and Zn allowing quantitative measurements of elemental concentration down to parts per million levels at the cellular level.

References

[1] R. Stocker, J.F. Keaney Jr., Phys. Rev. 84 (2004) 1381.
[2] S.H. Zhang, R.L. Reddick, J.A. Piedrahita, N. Maeda, Science 258 (1992) 468.
[3] C.A. Reardon, E.R. Miller, L. Blachowicz, J. Lukens, C.J. Binder, J.L. Witztum, G.S. Getz, J. Lipid Res. 45 (7) (2004) 1347, Jul.
[4] R.L. Reddick, S.H. Zhang, N. Maeda, Atherosclerosis 140 (1998) 297.
[5] B.J. Wu, K. Kathir, P.K. Witting, K. Beck, K. Choy, C. Li, K.D. Croft, T.A. Mori, D. Tanous, M.R. Adams, A.K. Lau, R. Stocker, J. Exp. Med. 203 (2006) 1117.
[6] B. Hennig, Y. Wang, S. Ramasamy, C.J. McClain, J. Nutr. 122 (1992) 1242.
[7] J. Clair, R. Talwalkar, C.J. McClain, B. Hennig, J. Trace Elem. Exp. Med. 7 (1995) 143.
[8] C. McClain, P. Morris, B. Hennig, Nutrition 11 (Suppl. 1) (1995) 117.
[9] J.H. Beattie, I.S. Kwun, Brit. J. Nutr. 91 (2) (2004) 177.
[10] M.Q. Ren, F. Watt, B.K.H. Tan, B. Halliwell, Free Radical Biol. Med. 34 (2003) 746.
[11] P.K. Witting, K. Pettersson, J. Letters, R. Stocker, Free Radical Biol. Med. 29 (2000) 295.
[12] F. Watt, J.A. van Kan, I. Rajta, A.A. Bettiol, T.F. Choo, M.B.H. Breese, T. Osipowicz, Nucl. Instru. and Meth. B 210 (2003) 14.
[13] R.S. Salzar, M.J. Thubrikar, R.T. Eppink, J. Biomechan. 28 (11) (1995) 1333.
[14] M.Q. Ren, R. Rajendran, N. Pan, B.K.H. Tan, F. Watt, B. Halliwell, Free Radical Biol. Med. 38 (2005) 1206.
[15] D. Ponraj, J. Makjanic, P.S.P. Thong, B.K.H. Tan, F. Watt, Febs Lett. 459 (1999) 218.
[16] G. Ku, N.S. Doherty, L.F. Schmidt, R.L. Jackson, R.J. Dinerstein, Faseb J. 4 (1990) 1645.
[17] M.Q. Ren, R. Rajendran, N. Pan, B.K.H. Tan, F. Watt, B. Halliwell, Free Radical Biol. Med. 41 (2006) 222.
[18] B.J. Wu, N. Girolamo, K. Beck, C.G. Hanratty, K. Choy, J.Y. Hou, M.R. Ward, R. Stocker. J. Pharmacol. Exp. Ther., in press.